AgroC

- A model for the simulation of carbon fluxes in agricultural ecosystems -

Documentation
Version 3.0

25 August 2022

Introduction

AgroC is a coupling between the SOILCO2/RothC model developed by Herbst et al. (2008) and the SUCROS model for crop growth (Spitters et al., 1989). The SOILCO2/RothC model simulates water, heat, and CO_2 flux in a soil column as well as the source term of heterotrophic respiration over soil depth and time, which is given by the turnover of depth-specific carbon pools (Coleman and Jenkinson, 2008; Šimůnek and Suarez, 1993; Šimůnek et al., 1996). The carbon turnover rate modifiers in turn are calculated according to the one-dimensional profiles of soil water content and temperature. This coupling concept was validated in several laboratory and field studies (Bauer et al., 2008, 2012; Herbst et al., 2008; Palosuo et al., 2012; Weihermüller et al., 2009). The extension of this coupled model with SUCROS was expected to allow for an improved simulation of the soil autotrophic respiration source term, since the temporal development of root growth and the related growth and maintenance respiration is simulated by SUCROS in a mechanistic way. Further, this allows to close the one-dimensional carbon balance and to estimate NEE, since carbon assimilation as well as organ-specific growth and maintenance respiration can be estimated.

The coupled SOILCO2/RothC model allows for the use of any user-specified length and time unit, whereas the SUCROS module uses fixed units. For the AgroC model we preserved the flexibility in terms of length ([L]) and time units ([T]), but we kept the fixed mass and area unit (kg, ha) of the original SUCROS code. The mass unit of the AgroC output carbon fluxes is mol CO_2.For a documentation related to all processes related to the original SoilCO2 model the user is referred to to Simunek et al. (1996). For plant growth as implemented in SUCROS the reader is referred to the WAVE manual (Vancloster et al., 1995) The following topics are documented here since modifications were performed or process sub-modules were added:

Contents

1. Hourly Time Step

The SOILCO2/RothC model can handle any time step, however the original SUCROS explicitly runs at a daily time step. Since particularly NEE exposes distinct diurnal variations, the SUCROS code was adopted to handle hourly time steps, except for the calculation of development stage DVS (-), for which the original parameterization, based on the effective temperature sum, was retained. In the original SUCROS approach the daily total gross assimilation is obtained by three point Gauss integration of the instantaneous assimilation rates per unit leaf area over the daylight period. This could be omitted for the hour model, for which the hourly gross assimilation is computed from the hourly average inputs of global radiation and mean temperature, based on the same approach that was originally used for the instantaneous assimilation rate. Major changes were, however, required for the estimation of the photosynthetic active radiation (PAR) flux at the top of the canopy. In the original code the instantaneous PAR (W $[L]^{-2}$) is estimated in dependence of *sinB* (-), the sine of solar inclination, and *dsinBE* (-), the daily integral of *sinB* including a correction of lower atmospheric transmittance at lower solar elevation. In the original day model the integral daily value *dsinBE* is approximated and *sinB* is estimated for the day of the year in dependence of the geographic position. For the hourly time steps, the integral of the sine of solar inclination *dsinB* is now calculated according to:

$$dsinB = sinB * 3600 \quad (1)$$

where 3600 is the number of seconds in one hour, instantaneous *sinB* (= $\sin(\delta)\sin(\varphi) + \cos(\delta)\cos(\omega)\cos(\varphi)$) is the sine of solar elevation, δ (°) is the sun declination angle, φ (°) is the geographic latitude and ω (°) is the hour angle. The value of *dsinBE* is then estimated as:

$$dsinBE = \sin(\arcsin(sinB) + 0.4\ sinB) * 3600 \quad (2)$$

where 0.4 is the regression coefficient between transmission and solar angle (Supit et al., 1994).

2. Water and heat Fluxes

Since the original approaches of SOILCO2 for water and heat flux were not modified in the coupled model, we describe them only briefly. The unsaturated soil water flux is described by the Richards equation:

$$\frac{\partial \theta}{\partial h}\frac{\partial h}{\partial t} = \frac{\partial}{\partial z}\left[k(h)\left(\frac{\partial h}{\partial z} - 1\right)\right] - Q \tag{3}$$

where t is the time [T], z is the vertical coordinate [L], θ is the volumetric water content [$L^3\ L^{-3}$], h is the pressure head [L], k is the unsaturated hydraulic conductivity [$L\ T^{-1}$] and Q is a source/sink term [T^{-1}]. The soil water capacity $\partial\theta/\partial h$ and the unsaturated hydraulic conductivity function k(h) are calculated according to Mualem-van Genuchten (van Genuchten, 1980). Soil heat transport is described by:

$$C_p(\theta)\frac{\partial T}{\partial t} = \frac{\partial}{\partial z}\left[\lambda(\theta)\frac{\partial T}{\partial z}\right] - C_w q_w \frac{\partial T}{\partial z} \tag{4}$$

where T is the soil temperature [K], λ is the apparent thermal conductivity [$W\ L^{-1}\ K^{-1}$], C_p is the volumetric heat capacity of the porous medium [$J\ L^{-3}\ K^{-1}$], C_w is the volumetric heat capacity of the soil water [$J\ L^{-3}\ K^{-1}$] and q_w is the water flux [$L\ T^{-1}$].

In terms of water fluxes, the coupling between SOILCO2 and SUCROS mainly covers two processes: rainfall interception and root water uptake. The interception loss is estimated according to the concept of an overflowing bucket (Rutter et al., 1971). For the estimation of canopy interception storage capacity S_i ([L]) at hourly time steps, it was assumed that S_i is proportional to the total leaf area index LAI ([$L^2\ L^{-2}$]) with $S_i = 0.2 \cdot LAI$. Water is removed from the interception storage by evaporation E_i ([$L\ T^{-1}$]):

$$E_i = \left(ET_{p,crop} - E_p\right)\frac{C_i}{S_i} \tag{5}$$

where C_i ([L]) represents the interception storage at a certain time step, $ET_{p,crop}$ ([L T^{-1}]) is the potential crop evapotranspiration, and E_p ([L T^{-1}]) is the potential soil evaporation. The amount of interception N_i ([L T^{-1}]) is then estimated according to:

$$N_i = \begin{cases} 0 & \text{for } N_0 = 0 \\ S_i - C_i & \text{for } S_i - C_i < N_0 \\ N_0 & \text{for } S_i - C_i > N_0 \end{cases} \quad (6)$$

where N_0 ([L T^{-1}]) represents the precipitation. Finally, the amount of precipitation entering the soil N_p ([L T^{-1}]) is calculated as the difference between N_0 and N_i.

In SUCROS $ET_{p,crop}$ is computed by scaling the potential grass reference evapotranspiration (Penman-Monteith approach; Allen et al., 1998) with the dimensionless crop conversion factor K_c.

K_c [-] can either be provided in a table in dependence of development stage DVS or in dependence of the day of the year DOY. Alternatively, K_c can be computed as a function of green leaf area index LAI_g [-]:

$$K_c = K_{c,min} + \frac{LAI_g}{LAI_{ref}\frac{1}{(1-K_{c,min})K_{c,sca}}} \quad (xx)$$

Where $K_{c,min}$ is the minimum allowed K_c during bare soil periods. The other input parameter is $K_{c,sca}$ which scales K_c over the growth period in dependence of LAI_g. LAI_{ref} (=2.88 according to Allen et al., 1998) is the leaf area index of the reference grass vegetation, used to estimate the potential grass reference evapotranspiration. $K_{c,min}$ should vary between 0.8 and 1, $K_{c,sca}$ varies between 1 and 10.

On the basis of Beer's law, $ET_{p,crop}$ is split into potential soil evaporation E_p ([L T^{-1}]) and potential transpiration T_p ([L T^{-1}]) in dependence of the LAI:

$$E_p = ET_{p,crop} \exp(-0.6 \cdot LAI) \quad (7)$$

$$T_p = ET_{p,crop} - E_p - E_i \quad (8)$$

The potential soil evaporation is passed to the water flux routine, where it prescribes the potential upward water flux for the upper boundary condition. Potential transpiration is distributed over the soil depth according to the relative root density distribution to provide the potential sink term of root water uptake over soil depth. The depth-specific actual root water uptake is computed by scaling the potential root water uptake with the reduction factor α (-) in dependence of soil pressure head h ([L]) following the approach of Feddes et al. (1978):

$$\alpha(h) = \begin{cases} \frac{h_0 - h}{h_0 - h_1} & h_0 \le h \le h_1 \\ 1 & \text{for} \quad h_1 \le h \le h_2 \\ 10^{\frac{h_2 - h}{h_3}} & h_2 \le h \le h_3 \end{cases} \quad (9)$$

where h_0, h_1, h_2, and h_3 ([L]) are prescribed threshold pressure heads (Vanclooster et al., 1995), which are plant dependent. Integrating the actual root water uptake over depth provides the actual transpiration T_a ([L T^{-1}]). The reduction of stomatal conductance due to water stress was assumed to correspond to the ratio between actual and potential transpiration T_a/T_p.

3. Carbon Fluxes from/to atmosphere

In this study the atmospheric convention is used. Downward carbon fluxes from the atmosphere to the ecosystem are defined as negative fluxes, and upward fluxes are positive.

The water stress ratio (T_a/T_p) is subsequently used to scale down gross carbon assimilation and to account for the effect of limited soil water availability on crop activity in terms of the negatively defined gross primary productivity *GPP* (mol CO_2 $[L]^{-2}$ $[T]^{-1}$):

$$GPP = -\frac{G_{phot}}{Mol_{CH_2O}} \cdot \frac{T_a}{T_p} \tag{10}$$

where G_{phot} (kg CH_2O $[L]^{-2}$ $[T]^{-1}$) is the glucose equivalent of the total gross assimilation per time step (Spitters et al., 1989), and Mol_{CH_2O} is the molar mass of CH_2O (= 0.030 kg mol^{-1}). The net primary productivity *NPP* (mol CO_2 $[L]^{-2}$ $[T]^{-1}$) is defined as:

$$NPP = GPP + R_{gr} + R_m \tag{11}$$

where R_{gr} (mol CO_2 $[L]^{-2}$ $[T]^{-1}$) is the total growth respiration, and R_m (mol CO_2 $[L]^{-2}$ $[T]^{-1}$) is the maintenance respiration. Net ecosystem exchange *NEE* (mol CO_2 $[L]^{-2}$ $[T]^{-1}$) is finally computed as:

$$NEE = NPP + R_h \tag{12}$$

where R_h (mol CO_2 $[L]^{-2}$ $[T]^{-1}$) is the depth-integral of the heterotrophic CO_2 source term provided by the RothC module.

4. Soil carbon fluxes

Transport of CO_2 in soil is simulated by considering diffusion J_{da} [L T^{-1}] and convection J_{ca} [L T^{-1}] in the gas phase, as well as dispersion J_{dw} [L T^{-1}] and convection J_{cw} [L T^{-1}] of CO_2 dissolved in the liquid phase:

$$\frac{\partial c_T}{\partial t} = -\frac{\partial}{\partial z}\left(J_{da} + J_{dw} + J_{ca} + J_{cw}\right) + S \tag{13}$$

where c_T [L^3 L^{-3}] is the total volumetric concentration of CO_2 and S [L^3 L^{-3} T^{-1}] is the production term of CO_2. The concentration of CO_2 in the liquid phase is assumed to be in instantaneous equilibrium with the gas phase concentration. The predominant transport process for CO_2 is the diffusion in the gas phase, calculated according to:

$$J_{da} = -\theta_a D_a \frac{\partial c_a}{\partial z} \tag{14}$$

where θ_a is the volumetric air content [L^3 L^{-3}], c_a is the volumetric CO_2 concentration in the gas phase [L^3 L^{-3}] and D_a is the effective soil matrix diffusion coefficient of CO_2 in the gas phase [L^2 T^{-1}]. This effective diffusion coefficient accounts for the tortuosity of the pore space and is calculated by the Millington-Quirk approach:

$$D_a = D_{as} \frac{\theta_a^{7/3}}{\theta_s} \tag{15}$$

where D_{as} is the diffusion coefficient of CO_2 in free air [L^2 T^{-1}] and θ_s is the saturated water content [L^3 L^{-3}]. The estimation of the CO_2 transport caused by air advection in the soil is based on a piston gas flow assumption, which implies that any water volume change in the soil profile must be immediately matched by a corresponding change in gas volume:

$$q_a(z) = q_w(0) - q_w(z) + \int_z^{L_r} Q(z)dz \tag{16}$$

where q_a is the soil air flux [L T^{-1}] and L_r is the length of the soil profile [L]. For a more detailed description of the CO_2 transport processes the reader is referred to the work of Šimůnek and Suarez (1993).

4.1 Production of CO_2

In the original version of the SOILCO2 model the total source term of CO_2 production S [L^3 L^{-3} T^{-1}] is the sum of the production by soil micro-organisms γ_S [L^3 L^{-3} T^{-1}] and plant roots γ_P [L^3 L^{-3} T^{-1}]:

$$S = \gamma_S + \gamma_P \tag{17}$$

The value of γ_s in the original SOILCO2 is calculated from an optimal CO_2 production rate γ_{s0} [L^3 L^{-2} T^{-1}], which is constant in time and distributed with an exponential function over the profile depth:

$$\gamma_s(z) = \gamma_{s0} a e^{-a(L_r - z)} \tag{18}$$

where L_r is the profile depth [L]. The exponential function is scaled with the constant *a* to ensure that the function is normalized according to the depth of the soil profile.

For the modified version of SOILCO2, the pool concept of the carbon turnover model RothC-26.3 (Coleman and Jenkinson, 2005) is used to estimate the CO_2 production by soil micro-organisms. It is assumed that soil organic matter (SOM) is composed of a variety of organic compounds, which are characterised by different decomposition rates. C-pools group substances with decomposition rates of the same order of magnitude. In the RothC model, SOM is partitioned into five compartments, where the inert organic matter pool (IOM) [M L^{-3}] is resistant to decomposition. The other four compartments are actively decomposed. These are the decomposable plant material (DPM) [M L^{-3}], the resistant plant material (RPM) [M L^{-3}], the microbial biomass (BIO) [M L^{-3}] and the humified organic matter (HUM) [M L^{-3}]. Incoming plant carbon is partitioned between DPM and RPM. Both DPM and RPM decompose to form CO_2, BIO and HUM. The partitioning between CO_2, BIO and HUM depends on the clay content of the soil using the following equation:

$$b = \frac{CO_2}{BIO + HUM} = 1.67(1.85 + 1.6e^{(-0.0786 clay 100)}) \tag{19}$$

where the clay fraction [M M^{-1}] is expressed on a gravimetric basis. The fraction of CO_2 carbon x_{CO2} [-] is thus equal to b/(b+1). Both BIO and HUM decompose to generate more CO_2, BIO and HUM. The ratio CO_2/(BIO+HUM) for the decomposition of BIO and HUM is the same as for the decomposition of DPM and RPM. The decomposition process is assumed to follow first-order kinetics:

$$\frac{\partial C_x}{\partial t} = C_x(-\lambda_x \prod_j f_j) \tag{20}$$

where the change of the concentration of any soil organic matter pool C_x [M L^{-3}] with time is characterised by the respective optimum decomposition rate λ_x [T^{-1}], which is scaled with the product of the reduction factors f_w for pressure head [-], f_T for temperature [-] and f_{CO2} for CO_2 concentration [-]:

$$\prod_j f_j = f_T f_W f_{CO_2} \tag{21}$$

For the decomposition of DPM and RPM, eq. (10) can be extended by the input from plant material C_{Pinp} [M L^{-3}]. This can be written in the discrete form as:

$$C_{p,i} = \left(C_{p,i-1} + y_{inp,x} C_{P\,inp,i-1}\right) e^{\left(-\lambda \prod_j f_j \Delta t\right)} \tag{22}$$

where C_p is the concentration of the pool [M L^{-3}], the index p loops over the fast pools DPM and RPM and $y_{inp,x}$ [-] = 0.59 for x=DPM and 0.41 for x =RPM (Coleman and Jenkinson, 2005), i is the index for the time increment and Δt is the length of the timestep [T]. The incoming carbon from plant material P_{in} [M L^{-2}] is distributed evenly across the soil up to a given depth D_p [L] to calculate the carbon input from plant material:

$$C_{Pinp} = \frac{P_{in}}{D_p} \tag{23}$$

Thus, the concentration of the decomposed carbon from DPM and RPM d_p [M L^{-3}] is equal to:

$$d_{p,i} = \left(C_{p,i-1} + y_{inp} C_{P\,inp,i-1}\right)\left[1 - e^{\left(-\lambda \prod_j f_j \Delta t\right)}\right] \tag{24}$$

The BIO and the HUM pool are charged by all active pools:

$$C_{s,i} = C_{s,i-1} e^{\left(-\lambda \prod_j f_j \Delta t\right)} + x_p \sum_{r=1}^{4} d_{r,i} \tag{25}$$

where x_p [-] is equal to $(1\text{-}x_{CO2})*0.45$ and $(1\text{-}x_{CO2})*0.54$ for BIO and HUM, respectively. Here, index s loops over the BIO and HUM pool, and index r loops over the four pools DPM, RPM, BIO and HUM. The concentration of the decomposed carbon from BIO and HUM d_s is equal to:

$$d_{s,i} = C_{s,i-1}\left[1 - e^{\left(-\lambda \prod_j f_j \Delta t\right)}\right] \tag{26}$$

Thus, the total mass concentration of CO_2 carbon [M L^{-3}] equals the sum of the CO_2 carbon produced from DPM, RPM, BIO and HUM:

$$C_{CO2-C,i} = x_{CO2} \sum_{r=1}^{4} d_{r,i} \tag{27}$$

The CO_2 mass concentration C_{CO2} [M L^{-3}] is calculated from the CO_2 carbon mass concentration $C_{CO2\text{-}C}$ [M L^{-3}] by scaling with the ratio between the molecular mass of CO_2 and C, which is 0.044 kg mol^{-1}/0.012 kg mol^{-1}. The CO_2 mass concentration is converted into a volumetric concentration assuming an ideal gas:

$$V_{CO2} = \frac{C_{CO2} R T}{M_{CO2} P} \tag{28}$$

where V_{CO2} is the volumetric CO_2 concentration [L^3 L^{-3}], R is the universal gas constant (=$6.2 \cdot 10^{14}$ kg cm^2 d^{-2} K^{-1} mol^{-1}) [M L^2 T^{-2} K^{-1} n^{-1}], T is the absolute temperature [K], M_{CO2} is the molar mass of CO_2 (=0.044 kg mol^{-1})[M n^{-1}] , and P is the atmospheric pressure (=$7.6 \cdot 10^{12}$ kg cm^{-1} d^{-2})[M L^{-1} T^{-2}]. The CO_2 production rate, which replaces the γ_s of the orginal approach in eq. (7), is calculated according to:

$$\gamma_s = \frac{V_{CO2}}{\Delta t} \tag{29}$$

The reduction of the CO_2 production as a function of the CO_2 concentration is based on Michaelis-Menten kinetics (Šimůnek and Suarez, 1993). The original SOILCO2 approach was slightly modified in order to obtain a value of 1.0 for optimum conditions:

$$f_{CO_2}(c_a) = \frac{0.21 - c_a}{0.42 - c_a - K^*_M} + 1 - \frac{0.21}{0.42 - K^*_M} \qquad \text{for} \qquad c_a < 0.21 \tag{30}$$

$$f_{CO_2}(c_a) = 0.0 \qquad \text{for} \qquad c_a \geq 0.21$$

where c_a is the CO_2 concentration [L L^{-3}] and K^*_m is the Michaelis` constant for the CO_2 concentration [L^3 L^{-3}], which was set to 0.19 cm^3 cm^{-3}.

The reduction factors for pressure head are calculated according to Šimůnek et al. (1996):

$$f_W(h) = 1.0 \qquad \text{for} \qquad h_1 \leq h \leq +\infty \tag{31}$$

$$f_W(h) = \frac{\log_{10}|h| - \log_{10}|h_2|}{\log_{10}|h_1| - \log_{10}|h_2|} \qquad \text{for} \qquad h_2 \leq h < h_1$$

$$f_W(h) = 0.0 \qquad \text{for} \qquad -\infty \leq h < h_2$$

where h_1 is the pressure head for optimum conditions [L], and h_2 is the pressure head below which CO_2 production ceases [L].

Compared to Šimůnek and Suarez (1993), the original Arrhenius-type temperature reduction function was shifted to obtain values of 1 for the RothC reference temperature T_{ref} [K] of 282.4 K:

$$f_r(T) = e^{\left[\frac{E(T - T_{ref})}{RTT_{ref}}\right]} \tag{32}$$

where T is the absolute temperature [K] and E is the reaction activation energy [M L^2 T^{-2} n^{-1}].

5. Maintenance and Growth Respiration

In a first step, the total maintenance respiration demand at 25°C $R_{m,r}$ (kg CH_2O $[L]^{-2}$ $[T]^{-1}$) is computed as a glucose equivalent according to:

$$R_{m,r} = \sum_{o=1}^{4} f_{m,o} W_o f_t \quad (33)$$

where $f_{m,o}$ (kg CH_2O kg^{-1} DM $[T]^{-1}$) is the maintenance coefficient with index o looping over the four plant organs leaves, stems, roots, and storage organs with values of 0.03, 0.015, 0.015, and 0.01, respectively (Spitters et al., 1989). W_o (kg DM $[L]^{-2}$) is the respective organ dry weight and f_t (-) is a time conversion factor accounting for the either hourly or daily time step. In the next step, $R_{m,r}$ is corrected for temperature to estimate total maintenance respiration $R_{m,c}$ (kg CH_2O $[L]^{-2}$ $[T]^{-1}$) as described by Spitters et al. (1989). In a last step, the CO_2 equivalent maintenance respiration R_m (mol CO_2 $[L]^{-2}$ $[T]^{-1}$) is computed as the quotient of $R_{m,c}$ and Mol_{CH_2O}.

Total growth respiration rate R_{gtot} (kg CH_2O $[L]^{-2}$ $[T]^{-1}$), again as the glucose equivalent, is estimated as:

$$R_{gtot} = \left(G_{phot} \cdot \frac{T_a}{T_p} - R_{m,c}\right) - \Delta W \cdot C_{cont} \cdot \frac{Mol_{CH_2O}}{Mol_C} \quad (34)$$

where ΔW is the overall dry matter growth rate (kg DM $[L]^{-2}$ $[T]^{-1}$), C_{cont} (g C g^{-1} DM) is the conversion factor between carbon and biomass dry matter weight, and Mol_C is the molar mass of C (= 0.012 kg mol^{-1}). Growth respiration for each plant organ $R_{gr,o}$ (mol CO_2 $[L]^{-2}$ $[T]^{-1}$) is computed from R_{gtot} according to:

$$R_{gr,o} = \frac{R_{gtot} \cdot f_o}{Mol_{CH_2O}} \quad (35)$$

where index *o* loops over the plant organs, and f_o (-) is the organ-specific partitioning factor also used to compute the organ-specific growth rate. Total growth respiration R_{gr} (mol CO_2 $[L]^{-2}$ $[T]^{-1}$) is finally computed as the sum of all $R_{gr,o}$. The sum of maintenance and growth respiration of the roots represents the autotrophic source term of soil CO_2 and was distributed over profile depth according to the time-variable relative root density distribution over depth.

6. Root Exudation and Root Decay

In SUCROS the daily or hourly glucose assimilation rate G_{phot} (kg CH_2O $[L]^{-2}$ $[T]^{-1}$) is partitioned in dependence of the DVS into the fraction for the shoot and for the root system to build up biomass. According to the labelling experiments performed by Swinnen et al. (1995) for winter wheat, 18.2% of the net assimilation are transferred to the roots, 7.1% are used to build up root biomass, and 5.3% are released as young photosynthetate rhizodeposition. In relation to the amount transferred to the roots this translates into relative fractions of 0.39 and 0.29 for root biomass and exudates, respectively. The relative root exudation fraction f_{exu} (-) thus equals 0.43 (= 0.29 / (0.39 + 0.29)) for winter wheat. In AgroC the root exudation rate Rt_{exu} (kg C $[L]^{-2}$ $[T]^{-1}$) is computed according to the above-mentioned constant partitioning factor from the dry matter root growth rate (kg DM $[L]^{-2}$ $[T]^{-1}$):

$$Rt_{exu} = \Delta W \cdot f_{rt} \cdot f_{exu} \cdot 0.467 \qquad (36)$$

where f_{rt} is the dimensionless partitioning coefficient for roots, and 0.467 kg C kg^{-1} DM is the root-specific dry matter carbon content (Goudriaan et al., 1997). This way, the root exudation shows diurnal variations in the simulations due to the assimilation rate as suggested by, e.g., Hopkins et al. (2013) and Kuzyakov (2006). Please note that the description of root exudation as documented above was implemented this way for all plant types when switched on (rootExudation=t). The relative root exudation fraction f_{exu} can be specified for each plant type in 'plants.in' at line 25.

Swinnen et al. (1995) also determined that 3.1% of the net assimilation ends up as dead roots. In relation to 18.2% transferred to the roots, this equals a relative fraction of 0.17. In order to account for the process of root death (rootDeath=t), the root death factor f_{dea} (-) was introduced. The basic assumption is that during the crop juvenile stages the root death rate is lower than at flowering:

$$f_{dea} = \begin{cases} 0 & DVS < 0.2 \\ \frac{f_{deamax}(DVS-0.2)}{0.5-0.2} & \text{for} \quad 0.2 \leq DVS \leq 0.5 \\ f_{deamax} & DVS > 0.5 \end{cases} \tag{37}$$

where f_{dea} is the death fraction in relation to the total amount of roots, and f_{deamax} (-) is the maximum value of the root death fraction (specified in line 26 of 'plants.in'). For the winter wheat model runs a f_{deamax} of 0.43 was used, which approximately reproduced the cumulative fraction of dead roots of 0.17 of net assimilation determined by Swinnen et al. (1995). Please note that root death is only implemented for winter wheat, summer wheat, barley and grassland. The rate of root death in terms of carbon release Rt_{dea} (kg C $[L]^{-2}$ $[T]^{-1}$) is computed as:

$$Rt_{dea} = \Delta W \cdot f_{rt} \cdot f_{dea} \cdot 0.467 \tag{38}$$

The root dry matter growth rate is reduced according to the loss of root exudates and dead roots. The total amount of root exudates and dead roots is, analogous to root respiration, distributed over depth according to the relative root density profile. The carbon equivalent of root exudates is transferred to the depth-specific decomposable plant material pool (DPM) of the RothC subroutine, in order to reflect the rapid decomposition of these labile substances by rhizosphere microorganisms, whereas the dead root carbon is split into the DPM pool and the resistant plant material pool (RPM) according to the original partitioning for incoming plant material of 0.59 and 0.41 (Coleman and Jenkinson, 2008), respectively.

For winter wheat and barley harvest residues can be considered in the simulation. At harvest the existing root biomass and 25% of the stem biomass is added to the DPM and RPM pool

up to a user-specified soil depth, i.e., ploughing depth. Figure 1 shows a schematic representation of the carbon cycling in AgroC.

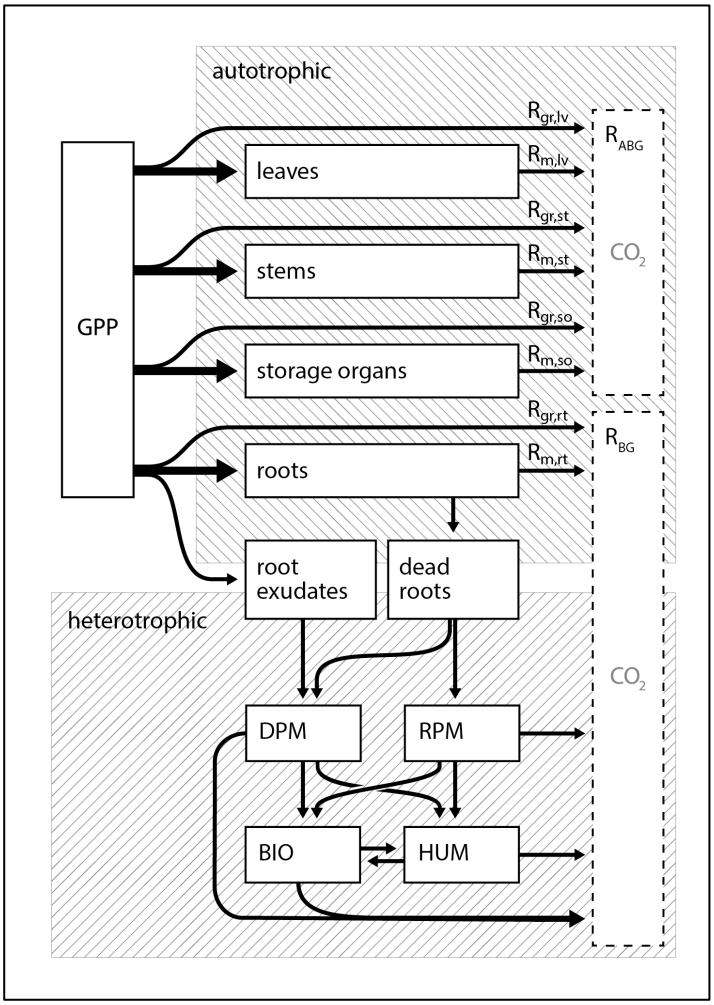

Fig. 1: Carbon fluxes and partitioning in AgroC. Gross primary production (GPP) is partitioned to the different plant organs, leaves (subscript lv), stems (st), storage organs (so), and roots (rt), whereat CO_2 is lost due to growth (R_{gr}) and maintenance respiration (R_m). The sum of these autotrophic CO_2 source terms by the shoot organs account for the above-ground respiration (R_{ABG}). Carbon or CO_2, respectively, is added to the soil profile by the autotrophic root respiration, root exudates, and dead roots. The latter two are transferred to the decomposable and resistant plant material pool (DPM, RPM) of the RothC model and decomposed. The heterotrophic CO_2 source term consists of the microbial decomposition of those and further soil organic matter pools (humified organic matter (HUM), microbial biomass (BIO)). The root respiration and the heterotrophic components are part of the below-ground respiration (R_{BG}).

7. Grassland

The original SUCROS code is not capable of simulating managed grassland, characterized by multiple mowing events over the season. Mowing initiates the transfer of glucose from the roots and the stubble to the remaining leaves, which allows for a faster compensation of defoliation. The routines implemented in AgroC for the simulation of the above-mentioned processes follow to some extent the sink/source approach suggested by Schapendonk et al. (1998) for the grassland productivity model LINGRA.

At prescribed mowing dates the current green leaf area index LAI_g is set to a fixed post-mowing leaf area index LAI_{post} of 0.35. The ratio between the pre-mowing LAI and post-mowing LAI_{post} is used to compute the respective loss of dry matter biomass:

$$f_{lai} = \frac{LAI_g}{LAI_{post}} \tag{39}$$

$$w_{post,i} = \frac{w_{pre,i}}{f_{lai}} \tag{40}$$

where f_{lai} (-) is the pre-/post-mowing LAI ratio, w_{pre} (kg DM $[L]^{-2}$) is the biomass prior to mowing, and w_{post} (kg DM $[L]^{-2}$) is the respective biomass after mowing. Index i loops over leaves, stems, and storage organs/inflorescence. At each mowing event DVS is also reset to a prescribed value of $DVS_{reset} = 0.5$. In order to simulate the transfer of glucose after defoliation, we implemented a glucose storage, which is filled between a DVS_{lo} of 0.6 and a DVS_{hi} of 1.0. The rate of glucose storage increase λ_{s+} (kg CH_2O $[L]^{-2}$ $[T]^{-1}$) is computed as a fraction f_{stor} (-) of global net glucose production:

$$\lambda_{s+} = \left(G_{phot} \cdot \frac{T_a}{T_p} - R_{m,c}\right) \cdot f_{stor} \tag{41}$$

The part of global net glucose production (= $G_{phot} \cdot T_a/T_p - R_{m,c}$) available for biomass growth and respiration is reduced accordingly by λ_{s+}. The storage fraction is computed in dependence of DVS:

$$f_{stor} = \begin{cases} 0 & DVS \leq DVS_{lo} \\ \frac{f_{stormax}(DVS - DVS_{lo})}{(DVS_{hi} - DVS_{lo})} & \text{for} \quad DVS_{lo} < DVS < DVS_{hi} \\ f_{stormax} & DVS \geq DVS_{hi} \end{cases} \tag{42}$$

where $f_{stormax}$ (-) is the user-specified maximum storage fraction. Thus, the glucose storage $S_{stor,t}$ (kg CH_2O $[L]^{-2}$) increases by λ_{s+} until a user-defined maximum value of $S_{stormax}$ (kg CH_2O $[L]^{-2}$) is reached and $S_{stor,t}$ remains constant. After mowing the glucose storage is emptied, assuming an exponential decay over time. The release of dry matter transfer rate λ_{s-} ($[T^{-1}]$) from $S_{stor,t}$ to the shoot is estimated as:

$$\lambda_{s-} = \frac{\log(100)}{t_{stor}} \tag{43}$$

where t_{stor} ([T]) is the user-specified time required to reach a value of 1% of the storage at the time of the mowing event. According to Gonzales et al. (1989) and Prud'homme et al. (1992) the mobilization of carbohydrates in ryegrass is highest during the first 6 days after defoliation and levelled out in a second phase, 6 to 29 days after cutting. As a default value, t_{stor} could be set to 15 days, equivalent to a λ_{s-} rate of 0.31 d^{-1}.

The additional dry matter growth rate ΔW_{stor} (kg DM $[L]^{-2}$ $[T]^{-1}$) resulting from the declining $S_{stor,t}$ is added to the dry matter growth rate of the shoot $\Delta W_{sh,}$ (kg DM $[L]^{-2}$ $[T]^{-1}$), which is the outcome of the photosynthetic activity of the plant. The additional shoot growth rate ΔW_{stor} is computed as:

$$\Delta W_{stor} = \frac{S_{stor,t}\ \lambda_{s-}}{f_{sh}\,(1.46\,f_{lv} + 1.51\,f_{st})} \quad (44)$$

where f_{sh}, f_{lv}, and f_{st} are the dimensionless partitioning factors for shoot, leaves, and stems, respectively. The assimilate requirement coefficients 1.46 and 1.51 have a unit of kg CH_2O kg^{-1} DM (Spitters et al., 1989). Correspondingly, $S_{stor,t}$ is reduced down to a limiting value of zero according to:

$$S_{stor,t+1} = S_{stor,t}\,(1 - \lambda_{s-}) \quad (45)$$

As suggested by Schapendonk et al. (1998) a mechanism was implemented by which the specific leaf area (ha leaf kg^{-1} DM) varies over the season as a function of DVS. Further, as proposed by Barrett et al. (2004) a mechanism to distinguish between vegetative and reproductive development of grass was appended. Those two stages of development differ in the productivity of the grass crop and in several major physiological processes, which alter the response of the plant to environmental drivers (e.g., Anslow and Green, 1967; Leafe et al., 1974; Parsons, 1988; Robson et al., 1988).

8. Root water uptake according to Couvreur

Alternatively to the Feddes approach, root water uptake can be simulated according to the approach of Couvreur et al. (2012) by setting waterstress=3 in the 'plants.in' input file. The weighted average total head in the root zone H_s (L) is computed as:

$$H_s = \sum_{j=1}^{n} RRD_j * H_j \quad (46)$$

where *RRD* is the relative root length density at node *j* [-] and *H* is the corresponding total hydraulic head (equal to $h+z$) and the entire soil profile is discretized into *n* nodes. The hydraulic head at the collar of the plant H_{col} is estimated at every time step as

$$H_{col} = -\frac{|T_p|}{K_{rs}} + H_s \quad (47)$$

where K_{rs} [cm^3 cm^{-3} T^{-1}] is the root system conductance and T_p [L T^{-1}] is potential transpiration. A threshold at the root collar H_{xmin} [L] is introduced (usually set to -16000 cm) and for $H_{col}<H_{xmin}$ the value of H_{col} is set equal to H_{xmin} and the actual transpiration T_a [L T^{-1}] is computed as:

$$T_a = K_{rs} * Max(0, H_s - H_{col}) \quad for\ H_{col} < H_{xmin} \quad (48)$$

For $H_{col} \geq H_{xmin}$ T_a is equal to T_p. Finally, the root water uptake in terms of the sink term *S* [T^{-1}] at node *j* is defined as:

$$S_j = \frac{RRD_j * \left(T_a + K_{comp} * \left(H_j - H_s\right)\right)}{dz_j} \quad (49)$$

where K_{comp} is the compensatory root conductance [T^{-1}] and dz [L] is the layer thickness related to node j.

9. Photosynthesis according to the big leaf approach (Farquhar)

The big leaf approach of Farquhar et al. (1980) as extended by Collatz et al. (1992) for C4 plants can be used alternatively to estimate photosynthesis (set farquhar=t in 'plants.in'). The atmospheric pressure P_{atm} [Pa], the ambient CO_2 partial pressure c_s [Pa], the oxygen partial pressure o_i [Pa], the CO_2 partial pressure at compensation point Γ_* [Pa], the maxiumum rate of carboylation V_{cmax} [µmol CO_2 m^{-2} s^{-1}] and the leaf internal CO_2 partial pressure c_i [Pa] are required to estimate photosynthesis. Further, quantum efficiency α was set to 0.06 µmol CO_2 µmol $photons^{-1}$ for C3 plants and it was assumed to be 0.04 µmol CO_2 µmol $photons^{-1}$ for C4 plants. (Note: For the units the area ('m^2') in this section always refers to the leaf area.)

Ambient CO_2 partial pressure c_s [Pa] is computed from the constant atmospheric CO_2 concentration and P_{atm} (both provided in the selector.in). O_2 partial pressure is calculated as $o_i=0.209*P_{atm}$.

In order to estimate the compensation point CO_2 partial pressure a Michaelis-Menten type approach is applied. The Michaelis-Menten constants K_c [Pa] and K_o [Pa], for CO_2 and O_2 respectively, are given as:

$$K_c = K_{c25}(a_{kc})^{\frac{t_a-25}{10}} \quad (50)$$

$$K_o = K_{o25}(a_{ko})^{\frac{t_a-25}{10}} \quad (51)$$

where K_{c25}=30 Pa and K_{o25}=30000 Pa at 25°C and a_{Kc}=2.1 and a_{Ko}=1.2, representing the relative change in K_{c25} and K_{o25} for a 10°C change of ambient temperature t_a. The compensation point CO_2 partial pressure [Pa] is subsequently estimated as:

$$\Gamma_* = 0.5 * \frac{K_c}{K_o} * 0.21 * o_i \quad (52)$$

In order to estimate V_{cmax}, first the temperature sensitivity factor $f(t_a)$ has to be estimated according to:

$$f(t_a) = \left[1 + exp\left(\frac{-220000+710*(t_a+t_f)}{0.001*R_{gas}*(t_a+t_f)}\right)\right]^{-1} \quad (53)$$

where t_f [K] is the freezing temperature of water and R_{gas} [J K^{-1} $kmol^{-1}$] represents the universal gas constant. This also accounts for the thermal breakdown of carbon assimilation due to freezing. In the next step V_{cmax} [µmol CO_2 m^{-2} s^{-1}] is computed from $V_{cmacx25}$ [µmol CO_2 m^{-2} s^{-1}] (plant specific input parameter) scaled by $f(t_a)$ [-], root water uptake stress α_{avg} [-] ($=T_a/T_p$) and relative day length $f(DYL)$ [-]:

$$V_{cmax} = V_{cmax25} * (2.4)^{\frac{t_a-25}{10}} * f(t_a) *\propto_{avg}* f(DYL) \quad (54)$$

As implemented in SCOPE, the leaf internal CO_2 partial pressure c_i [Pa] was estimated as:

$$\begin{aligned} c_i &= Maximum\left(\Gamma_*, c_s * \left(1 - 1.6/\left(m * R_h * \alpha_{avg}\right)\right)\right) && for\ C3\ plants \\ c_i &= Maximum\left(0.99 * P_{atm}, c_s * \left(1 - 1.6/\left(m * R_h * \alpha_{avg}\right)\right)\right) && for\ C4\ plants \end{aligned} \quad (55)$$

where m [-] is the Ball-Berry slope parameter (Collatz et al., 1991; plant specific input parameter) and R_h [-] is the relative humidity (last column in 'atmosph.in').

Photosynthesis A [µmol CO_2 m^{-2} s^{-1}] of C3 plants is finally estimated as:

$$A = Minimum\left(\frac{V_{cmax}*(c_i-\Gamma_*)}{c_i+K_c*(1+o_i/K_o)}, \frac{(c_i-\Gamma_*)*4.6*APAR*\alpha}{c_i+2*\Gamma_*}, V_{cmax} * 0.5\right) \quad (56)$$

whereas the photosynthesis of a C4 plants is finally estimated as

$$A = Minimum\left(V_{cmax}, 4.6 * APAR * \alpha, 4000 * V_{cmax} * \frac{c_i}{P_{atm}}\right) \quad (57)$$

The single terms of the minimum functions represent the RuBP carboxylase limited rate of carboxylation, the light-limited rate and the export limited rate of carboxylation (from left to right).

10. Solar induced fluorescence SIF

SIF was basically estimated following the concept of Lee et al. (2015). The maximum possible electron transport rate J_o [µmol CO_2 m^{-2} s^{-1}] was computed according to

$$J_o = 4.6 * APAR * \alpha \quad (58)$$

where the photosynthetic active radiation APAR [W m^{-2} = J m^{-2} s^{-1}] is scaled with 4.6 µmol photons $Joule^{-1}$ to convert to photosynthetic photon flux and with quantum efficiency α (=0.06 µmol CO_2 µmol $photons^{-1}$ for C3 and =0.04 for C4 plants) to convert to CO_2 flux. The actual electron transport rate J_e of C3 plants is given by

$$J_e = A * \frac{c_i + 2*\Gamma_*}{c_i - \Gamma_*} \quad (59)$$

where A [µmol CO_2 m^{-2} s^{-1}] is the actual photosynthesis rate, c_i [Pa] represents the leaf internal CO_2 partial pressure and Γ_* [Pa] is the CO_2 partial pressure at compensation point. For C4 plants J_e is equal to A. The photochemical quantum yield ϕ_p [-] is estimated from

$$\phi_p = \phi_{po} * \frac{J_e}{J_o} \quad (60)$$

where ϕ_{po} [-] is the efficiency of photochemical trapping in the dark-adapted state. According to Björkman and Demmig (1987) the typical value of ϕ_{po} for a healthy plant is 0.8. The rate coefficient of chlorophyll fluorescence k_f is set to 0.05 s^{-1}, whereas the dark adapted rate coefficient k_d [s^{-1}] is estimated in dependence of ambient temperature t_a [°C]:

$$k_d = Maximum(0.03 * t_a + 0.0773, 0.087) \quad (61)$$

The light adapted rate coefficient k_n [s^{-1}] was estimated as

$$k_n = (6.2473 * x - 0.5944) * x \quad (62)$$

where x is equal to $1-\phi_p/\phi_{po}$. Fluorescence yield ϕ_f[-] is subsequently computed as

$$\phi_f = \frac{k_f}{k_f+k_d+k_n} * (1 - \phi_p) \quad (63)$$

Leaf level sun induced fluorescence F [µmol photons m^{-2} s^{-1}] is

$$F = \phi_f * APAR * 4.6 \quad (64)$$

Following Lee et al. (2015) leaf-level fluorescence can be converted to spectrometer-measured fluorescence at 755 nm F_{755nm} using the conversion factor k which accounts for the integration over all wavelengths in the fluorescence emission spectrum, observing angle and unit conversion from µmol photons m^{-2} s^{-1} to W m^{-2}:

$$F_{755nm} = \frac{F}{k} \quad (65)$$

An empirical step-wise linear relation between k and V_{cmax25} [µmol CO_2 m^{-2} s^{-1}] is finally used to compute the conversion factor (Lee et al., 2015):

$$k = 0.047716 * V_{cmax25} + 7.70092 \quad for \quad V_{cmax25} \leq 70$$
$$k = 0.032686 * V_{cmax25} + 8.75302 \quad for \quad V_{cmax25} > 70 \tag{66}$$

11. CO_2 diffusion coefficients

The diffusion coefficient of CO_2 in the porous system D_a [L^2 T^{-1}] is computed from the temperature dependent CO_2 diffusion coefficient in free air D_{as} [L^2 T^{-1}] and the air-filled porosity θ_a [cm^3 cm^{-3}]. Alternatively to the originally implemented Millington-Quirk approach (iGasdiff=1), the approach of Kristensen et al. (2010) accounting for diffusion in macropores can be applied (set iGasdiff=5):

$$D_a = \begin{cases} D_{as} * H * \theta_a & for\ \theta_a < \varepsilon^* \\ D_{as} * \left(H * \varepsilon^* + (\theta_a - \varepsilon^*)^{X_m} \left(\frac{\theta_a - \varepsilon^*}{\theta_s - \varepsilon^*} \right) \right) & for\ \theta_a > \varepsilon^* \end{cases} \quad (67)$$

where H is the macropore tortuosity factor [L L^{-1}], X_m is the matrix tortuosity factor [L L^{-1}], θ_s [cm^3 cm^{-3}] is the water content at saturation (assumed to be equal to porosity) and $\varepsilon*$ is the macropore porosity [cm^3 cm^{-3}]. In relation to Millington-Quirk, this allows for higher diffusion coefficients near water saturation. Three parameters are required as input for each material: ε∗, H and X_m.

Further, diffusion coefficients can be estimated according to Moldrup et al. (2000a, iGasdiff=2) for repacked soils, according to Moldrup et al. (2000b, iGasdiff=3) and according to a double-linear approach (iGasdiff=4).

12. Nitrogen

The AgroC nitrogen module accounts for the carbon turnover-linked mineralization and immobilization of soil organic N, nitrification, denitrification, Urea hydrolysis, Ammonia volatilization, N_2O emission, N fixation and crop demand-driven uptake by roots. Further, in combination with the solute transport routine Ammonium sorption, convective-dispersive transport and leaching of Ammonium and Nitrate can be accounted for (see Fig. X).

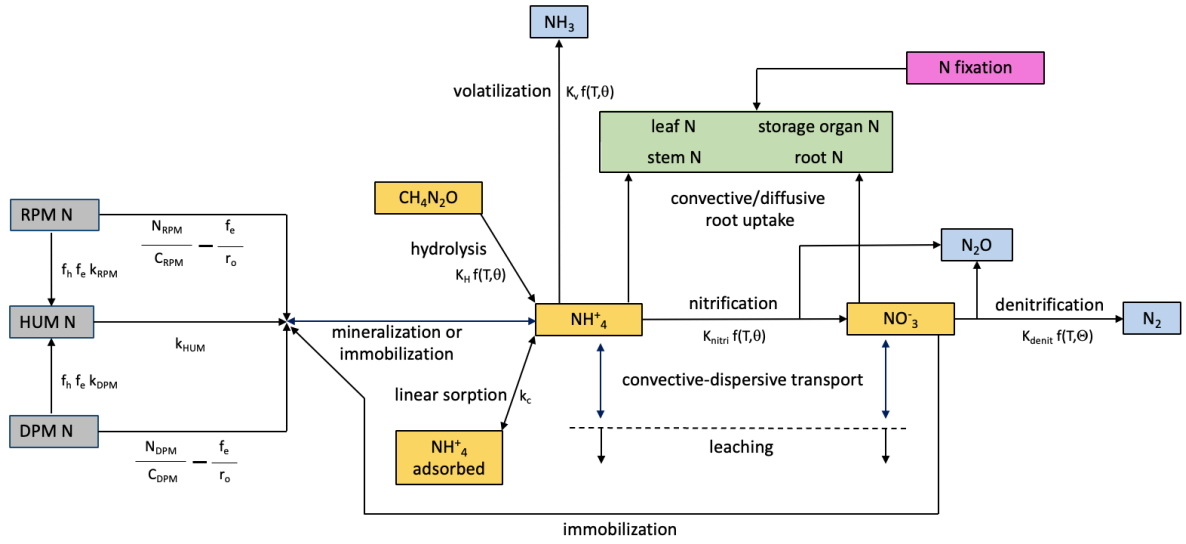

Fig. 2: AgroC nitrogen cycle as a combination of RothC (Coleman & Jenkinson, 2014) and SWATNIT (Vereecken et al., 1991)

12.1 Mineralization of soil organic nitrogen

The potential rate constants of the organic matter pools are specified as input in the carbon turnover section. The actual turnover rates are consistently used for the decomposition of organic C, N and P. Actual turnover rates are calculated from the potential rate constants in dependence of soil temperature, water content (or pressure head) and aeration, as described in section 4, Eqs. 20 to 22. The organic nitrogen pool structure follows the structure of the RothC pool concept applied for the organic C turnover, except for the BIO pool. This pool explicitly accounts for the carbon stored in the biomass and is for the organic nitrogen

turnover replaced with a fixed biomass C/N ratio provided as model input. The decomposition of organic N in the decomposable (DPM) and in the resistant plant material (RPM) as well as in the humus pool (HUM) is estimated as follows:

$$\frac{\partial N_{DPM}}{\partial t} = \left[(1 - f_h) f_e \frac{1}{r_o} - \frac{N_{DPM}}{C_{DPM}}\right] C_{DPM} \lambda_{DPM} \quad (68)$$

where N_{DPM} [M N L^{-3} soil] is the nitrogen content in the decomposable plant material DPM pool, C_{DPM} [M C L^{-3} soil] is the carbon content of the DPM pool, λ_{DPM} [T^{-1}] is the DPM turnover rate and r_o [-] represents the biomass C/N ratio. For consistency with the RothC estimated carbon turnover, the dimensionless turnover efficiency f_e [-] is computed as 1-b/(b+1) (see Eq. 9, section 4.1), and the dimensionless humification facor f_h is equal to 0.54 (=RothC humification factor, please also see Eq. 15). A similar nitrogen turnover loop is assumed for the resistant plant material pool:

$$\frac{\partial N_{RPM}}{\partial t} = \left[(1 - f_h) f_e \frac{1}{r_o} - \frac{N_{RPM}}{C_{RPM}}\right] C_{RPM} \lambda_{RPM} \quad (69)$$

where N_{RPM} [M N L^{-3} soil] is the nitrogen content in the RPM pool, C_{RPM} [M C L^{-3} soil] is the carbon content of the RPM pool and λ_{RPM} [T^{-1}] is the RPM turnover rate. The net increase rate of nitrogen in the humus pool N_{HUM} [M N L^{-3} soil] is given by:

$$\frac{\partial N_{HUM}}{\partial t} = \frac{f_e f_h}{r_o} (C_{DPM} \lambda_{DPM} + C_{RPM} \lambda_{RPM}) - C_{HUM} \lambda_{HUM} \quad (70)$$

Where C_{HUM} [M C L^{-3} soil] is the carbon content of the HUM pool and λ_{HUM} [T^{-1}] is the HUM turnover rate. The C and N turnover may result in net production or consumption of

Ammonium, which depends on the biomass C/N ratio and the C/N ratio of the three pools organic matter pools. The decrease of soil organic N in the three pools due to mineralization equals the increase of nitrogen in the form of Ammonia N_{NH4} [M N L^{-3} soil]:

$$\frac{\partial N_{NH4}}{\partial t} = \left[\frac{N_{DPM}}{C_{DPM}} - \frac{f_e}{r_o}\right] C_{DPM}\lambda_{DPM} + \left[\frac{N_{RPM}}{C_{RPM}} - \frac{f_e}{r_o}\right] C_{RPM}\lambda_{RPM} + C_{HUM}\lambda_{HUM} \quad (71)$$

The Ammonia-N is converted to the mass of NH_4 and to a liquid phase concentration to be used as a source/sink term [M NH_4 L^{-3} water T^{-1}] in the solute transport equation. When the right side of the equation above is positive, mineralization occurs. In case the right side is negative immobilization occurs and nitrogen mass is transferred from the liquid phase to the organic matter nitrogen pools. If immobilization occurs and the liquid phase concentration of NH_4 is not sufficient to fulfill the mineralization N demand, liquid phase NO_3 is transferred to the organic N pools. If also the Nitrate supply to the mineralization process is not sufficient, λ_{DPM} and λ_{RPM} are reduced by the supply/demand ratio. For the supply from the liquid phase N, the N_{DPM} pool is prioritized to the N_{RPM} pool, i.e. the remaining liquid phase Ammonium and/or Nitrate may be consumed by the N_{DPM} decomposition first. The potentially decreased λ_{DPM} and λ_{RPM} rates are also used in the organic C and P mineralization module. Thus, a nitrogen gap in the organic N mineralization of one or both plant material pools will likewise reduce the decomposition of the respective plant material C and P pools. Eqs. 68 to 71 are solved numerically by application of the Euler integration method.

12.2 Nitrification, Ammonia volatilization and Urea hydrolysis

In the nitrification process Ammonium is transformed to Nitrate by heterotrophic microorganisms. A first order kinetic equation, based on an actual nitrification rate is applied, where the actual nitrification rate is computed from a potential nitrification rate λ_{nitri} [T^{-1}]

specified as input. The potential nitrification rate is scaled with the rate modifiers accounting for soil temperature and water content also used for the organic decomposition rate scaling. Ammonium sorbed to the soil matrix is not transformed to Nitrate, this only occurs for the dissolved Ammonium.

Ammonia volatilization is again described by a first order kinetic approach, where the actual volatilization rate is computed from the potential volatilization rate λ_{vol} [T^{-1}] scaled by the rate modifiers for soil temperature and water content.

Hydrolysis of Urea, as a basic constituent in many mineral N fertilizers, is also described with a first order kinetic reaction. Again, soil water content and soil temperature affect the potential hydrolysis rate λ_{hyd} [T^{-1}].

12.3 Denitrification

Denitrification is simulated as a first order kinetic reaction, where the liquid phase Nitrate concentration NO_3 [M NO_3 L^{-3} water] is denitrified according to the actual denitrification rate $\lambda_{a,denit}$ [T^{-1}]:

$$\frac{\partial NO_3}{\partial t} = NO_3 \lambda_{a,denit} \tag{72}$$

The actual denitrification rate is computed from the potential denitrification rate λ_{denit} [T^{-1}], given as input, and it is scaled with the common rate modifier for soil temperature. However, the rate modifier for soil water content $f_{w,denit}$ [-] differs from the soil water content rate modifier used for all the other turnover rates in order to account for the effect of soil aeration:

$$f_{w,denit} = 0 \qquad for\ \Theta_e \leq \theta_d$$

$$f_{w,denit} = \left(\frac{\Theta_e - 0.8}{0.2}\right)^2 \quad for\ \Theta_e > \theta_d \tag{73}$$

Where θ_d [L^3 L^{-3}] is a threshold water content, set to 0.8 according to Aulakh et al., 1992), Θ_e is the effective saturation [-] and θ_s [L^3 L^{-3}] is the water content at saturation.

12.4 Root uptake of nitrogen

The uptake scheme follows the approach suggested by McIsaac et al. (1985), which was modified by Huwe and van der Ploeg (1988).

The potential uptake (=demand) N_p [M N L^{-2}] is is computed from a dry matter nitrogen concentration for each crop organ, as provided in the plant parameter input file against development stage DVS. Total potential uptake rate dN_p/dt [M N L^{-2} T^{-1}] is defined the sum of the following organ-specific potential uptake rates:

$$\frac{\partial N_p}{\partial t} = \frac{\partial N_{lea}}{\partial t} + \frac{\partial N_{ste}}{\partial t} + \frac{\partial N_{roo}}{\partial t} + \frac{\partial N_{crn}}{\partial t} \quad (74)$$

Where N_{lea}, N_{ste}, N_{roo} and N_{crn} [M N L^{-2}] represent the nitrogen demand of leaves, stems, storage organs, roots and crowns respectively. The potential uptake rate of each plant organ is computed as:

$$\frac{\partial N_i}{\partial t} = W_i * XNC_i - N_{act,i} \quad (75)$$

Where W_i [M DM L^{-2}] is the accumulated dry matter, XNC_i [M N M^{-1} DM] is the potential dry matter nitrogen concentration of the crop organs, $N_{act,i}$ [M N L^{-2}] is the nitrogen accumulated in the organ and index *i* loops over leaves, stems, storage organs and roots. Uptake is supposed to occur convective, with the root water uptake, and diffusive. Potential convective uptake rate [M N T^{-1}] is given by:

$$\frac{\partial N_{conv}}{\partial t} = \int_0^{R_d} S_w * C_m * dx \quad (76)$$

Where R_d is actual root depth [L], *dx* is the element thickness [L], C_m is the liquid phase concentration of either Nitrate [M NO_3 L^{-3} water] or Ammonia [M NH_4 L^{-3} water] and S_w [L^3 L^{-3} T^{-1}] is the root water uptake sink term. The nitrogen uptake is simulated as a sink term in the solute transport routine, where uptake could never exceed the available liquid phase nitrogen mass. Ammonium will only be taken up, when the crop Nitrogen demand exceeds Nitrate supply. Only when convective uptake is smaller than the potential uptake, a potential diffusive uptake is calculated as the difference between potential and convective uptake. Actual diffusive uptake N_{dif} [M N L^{-2}] is calculated as:

$$\frac{\partial N_{dif}}{\partial t} = \int_0^{R_d} \frac{2*\pi*R_{dens}*RORAD*\tau*C_m*\theta}{D_0} dx \quad (77)$$

Where R_{dens} [L L^{-3}] is root density at a specific depth, RORAD [L] is the mean root radius, τ [L^2 T^{-1}] is the solute diffusion coefficient for a given water content, D_0 [L^{-1}] is the travel distance resistance between bulk soil solution and root, C_m is the liquid phase concentration of either Nitrate [M NO_3 L^{-3} water] or Ammonia [M NH_4 L^{-3} water] and dx is the depth increment [L]. Please note that the uptake rates N_{dif} and N_{conv} are related to soil volume, and not to water volume. Root density over depth is calculated by scaling the root density at the surface W_{0dens} [L L^{-3}] with the relative root density RRD [-].

The organ-specific actual root Nitrogen uptake dRNUP$_{act,i}$/dt [M N L^{-2}], where index i again loops over leaves, stems, storage organs and roots is given as:

$$\frac{\partial RNUP_{act,lea}}{\partial t} = \frac{\partial N_{lea}}{\partial t} * \frac{\frac{\partial N_{conv}+\partial N_{dif}}{\partial t}}{\frac{\partial N_p}{\partial t}} - \frac{\partial N_{so}}{\partial t} * \left(\frac{W_{lea}}{W_{lea}+W_{ste}}\right) \quad (78)$$

$$\frac{\partial RNUP_{act,ste}}{\partial t} = \frac{\partial N_{ste}}{\partial t} * \frac{\frac{\partial N_{conv}+\partial N_{dif}}{\partial t}}{\frac{\partial N_p}{\partial t}} - \frac{\partial N_{so}}{\partial t} * \left(\frac{W_{ste}}{W_{lea}+W_{ste}}\right) \quad (79)$$

$$\frac{\partial RNUP_{act,roo}}{\partial t} = \frac{\partial N_{roo}}{\partial t} * \frac{\frac{\partial N_{conv}+\partial N_{dif}}{\partial t}}{\frac{\partial N_p}{\partial t}} \quad (80)$$

$$\frac{\partial RNUP_{act,so}}{\partial t} = \frac{\partial N_{so}}{\partial t} = (W_{so} * XNC_{so} - N_{so}) * FN_{def} \quad (81)$$

$$FN_{def} = 1 - \sqrt{1 - N_{RED}{}^2} \quad (82)$$

Where FN_{def} [-] describes the reduction of N transfer to the storage organs according to a potential limitation of N uptake.

The overall reduction of growth N_{RED} [-] according to Nitrogen limitation is described with a dimensionless reduction factor, varying between 0 and 1:

$$N_{RED} = \left(\frac{ANCL-RLNCL}{RMNCL-RLNCL}\right) \quad (83)$$

Where ANCL [kg N kg^{-1} DM], is the actual tissue nitrogen concentration of the leaves, RMNCL [kg N kg^{-1} DM] is a leaf nitrogen threshold value for unrestricted growth assumed to be 50% of XNC_{LE} and RLNCL represents the leaf nitrogen threshold concentration below which growth ceases. Latter is fixed to 0.005 [M N M^{-1} DM].

The effect of stressors, each varying between 0 and 1, on photosynthesis is assumed to follow the minimum concept:

$$GA_{t,a} = GA_{t,p} * Min(\propto_{avg}, N_{RED}, P_{RED}) \quad (84)$$

Where $GA_{t,a}$ [M CH_2O L^{-2} T^{-1}] is the actual total gross assimilation, $GA_{t,p}$ [M CH_2O L^{-2} T^{-1}] is the potential total gross assimilation, α_{avg} [-] is the stress factor accounting for water stress, defined as T_a/T_p, and P_{RED} [-] is the stressor potentially accounting for limitations in phosphorus uptake (see Eq. 96).

12.5 Nitrogen fixation

Symbiosis between some grass species and leguminous crops with rhizobia allow for the direct supply of plants with N taken up from the soil air. In a first step an optimum N fixation rate $\lambda_{fix,opt}$ [M N L^{-2} T^{-1}] is given as model input. Typically $\lambda_{fix,opt}$ is in the range of 0.1 to 1 kg N ha^{-1} d^{-1}. Since N fixation is a bacterial process abiotic state variables affect the actual N fixation rate $\lambda_{fix,act}$ [M N L^{-2} T^{-1}] . In order to account for abiotic stresses on N fixation a root density and element thickness weighted average reduction factor f_{mean} [-] resulting from the distribution of soil temperature, soil water content and soil aeration over depth is computed:

$$f_{mean} = \sum_{n}^{i=1} f_{T,i} f_{w,i} f_{CO2.i} \frac{RRD_i + \partial z_i / R_d}{2} \qquad \text{(Eq. 85)}$$

Where $f_{T,i}$ is the dimensionless reduction factor according to soil temperature (Eq. 32), $f_{w,i}$ [-] is the reduction factor according to water content (Eq. 31), $f_{CO2,I}$ [-] is the reduction factor according to soil CO_2 concentration (Eq. 30), RRD_i [-] is the relative root density, dz_i is the element thickness [L] at node i, R_d is the actual root depth [L] and n is the number of nodal points. Note that in dependence of the reference temperature applied the reduction factor for temperature could actually be larger than 1, whereas all other reduction factors vary between 0 and 1. In order to account for the effect of the temporal evolution of the root system on the actual N fixation rate the ratio between R_d and maximum rooting depth R_{dmax} [L] is computed:

$$f_{Rd} = \frac{R_d}{R_{dmax}} \quad \text{(Eq. 86)}$$

Where f_{Rd} [-] is the reduction factor according to the root system development. Assuming that a potential N deficit in the plant, as a consequence of limited N supply from the soil, will foster root carbon supply to the rhizobia and an increase in N fixation, the factor accounting for the effect of N limitation (Eq. 83) on N fixation f_N [-] is computed as:

$$f_N = 1 + 1 - N_{RED} \quad \text{(Eq. 87)}$$

The actual N fixation rate is subsequently computed as:

$$\lambda_{fix,act} = \lambda_{fix,opt} f_{mean} f_{Rd} f_N f_{col} \quad \text{(Eq. 88)}$$

Where f_{col} is the dimensionless crop specific rhizobia colonization fraction (= nodulation ratio), which is assumed to be one for C3 and C4 grass and zero for all other crop types. The actual N fixation rate is split up into the fractions of N shifted to each plant organ according to the organ-specific N demand. N fixation is not allowed to exceed the plant N demand. The total potential N root uptake rate [M N L^{-2} T^{-1}] is computed as total plant N demand rate [M N L^{-2} T^{-1}] minus actual N fixation rate.

12.6 Production of soil N_2O emissions

Following the 'hole-in-the-pipe' approach of Firestone & Davidson (1989), a production of N_20 with a constant fraction of 0.06% (Lin et al., 2000) accompanying nitrification is assumed:

$$R_{N2Onit} = 0.0006\, R_{nit}\, \frac{44}{18} \quad \text{(XX)}$$

Where R_{N2Onit} [M N_2O L^{-3} soil T^{-1}] is the N_2O production during nitrification, R_{nit} [M NH_4 L^{-3} soil T^{-1}] is the actual nitrification rate and 44/18 is the molar mass ratio of N_20/NH_4. N_20 production during denitrification is computed as:

$$R_{N2Odenit} = R_{denit} F_{N2N2O} \frac{44}{62} \quad \text{(XX)}$$

Where $R_{N2Odenit}$ [M N_2O L^{-3} soil T^{-1}] is the N_2O production rate during denitrification, R_{denit} [M NO_3 L^{-3} soil T^{-1}] is the actual denitrification rate, F_{N2N20} [-] is the fraction of NO_3 that is transformed to N_2O and not to N_2 and 44/62 is the molar mass ratio of N_2O/NO_3. According to del Grosso et al. (2000) F_{N2N20} can be estimated as:

$$F_{N2N2O} = 1/(1 + \max(0.16\, k_1, k_1\, exp^{(-0.8\, P_{NO3CO2})})\, f_{WFPS}) \quad \text{(XX)}$$

Where according to del Grosso et al. (2000) P_{NO3CO2} is the ratio of NO_3 concentration [M NO_3 L^{-3}] to CO_2 production [M CO_2 L^{-3} day^{-1}] accounting for the ratio of electron donor to substrate, k_1 [-] is a parameter controlling the maximum value of the N_2/N_20 ratio in dependence of relative gas diffusivity and f_{WFPS} is a parameter describing the response of the N_2/N_2O ratio to soil water-filled pore space given as:

$$k_1 = \max(1.7, 38.4 - 350\, \tau_a) \quad \text{(XX)}$$

$$f_{WFPS} = \max(0.1, 1.5\, \Theta_e - 0.32) \quad \text{(XX)}$$

Where τ_a [-] is the relative diffusion coefficient, or pore tortuosity computed e.g. according to the Millington-Quirk approach, also used to scale the CO_2 diffusion coefficient in free air (see

section 11 or Eq.15) and Θ_e [-] is the effective saturation (=WFPS) given as $(\theta-\theta_r)/(\theta_s-\theta_r)$. Please note that the relative diffusion coefficient is always consistently used with the relative diffusion computation method (igasdiff = 1 to 5) chosen for CO_2 diffusion.

Total soil N_20 production R_{N2O} [M N_2O L^{-3} soil T^{-1}] is the sum of N_20 produced within the nitrification process and within the denitrification process. Multiplication of R_{N2O} with element thickness *dx* [L] and summing up over the entire soil profile gives the total soil N_2O emission [M N_2O L^{-2} soil T^{-1}], assuming all N_20 produced in the profile is transported to the soil surface within the timestep. Please note that the timing of the N_2O production largely depends on the threshold water content of 0.8 used for the denitrification reduction (see Eq. 72) and that the absolute magnitude largely depends on the actual denitrification rate as computed from the optimum denitrification rate and the soil temperature reduction factor.

13. Phosphorus

The AgroC phosphorus sub-module accounts for organic and mineral fertilization, the mineralization of organic phosphorus, the convective-dispersive transport and sorption of mineral phosphorus and the uptake of liquid-phase phosphorus (Fig. 3).

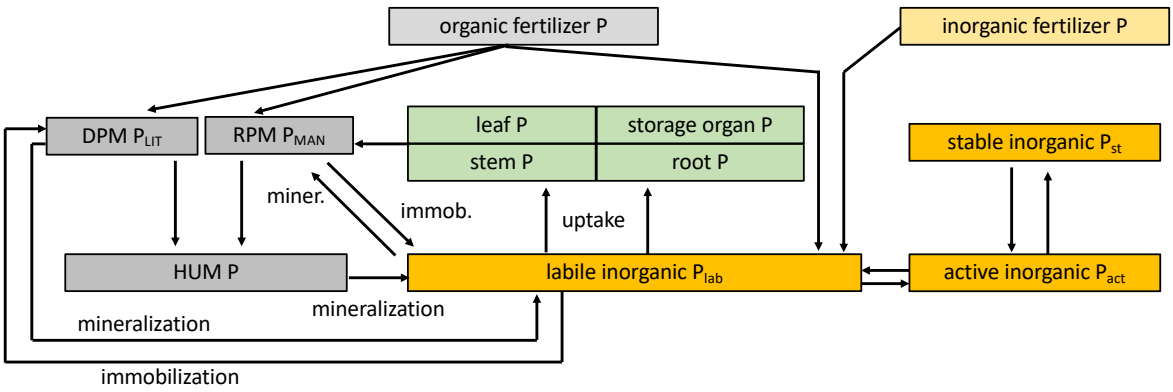

Fig. 3: Schematic representation of the phosphorus cycling as implemented in AgroC

13.1 Mineralization of soil organic phosphorus

As already mentioned in section 11.1: The actual turnover rates are used in a consistent manner for the decomposition of organic C, N and P. Rate modifiers are applied as described in section 4, Eqs. 20 to 22. The organic phosphorus pool structure follows the structure of the pool concept for nitrogen (see Fig. 4). The turnover of the organic Phosphorus is again closely linked to turnover of organic carbon, however a fixed biomass C/P ratio, provided as model input, again replaces the biomass pool used in the RothC carbon turnover approach.

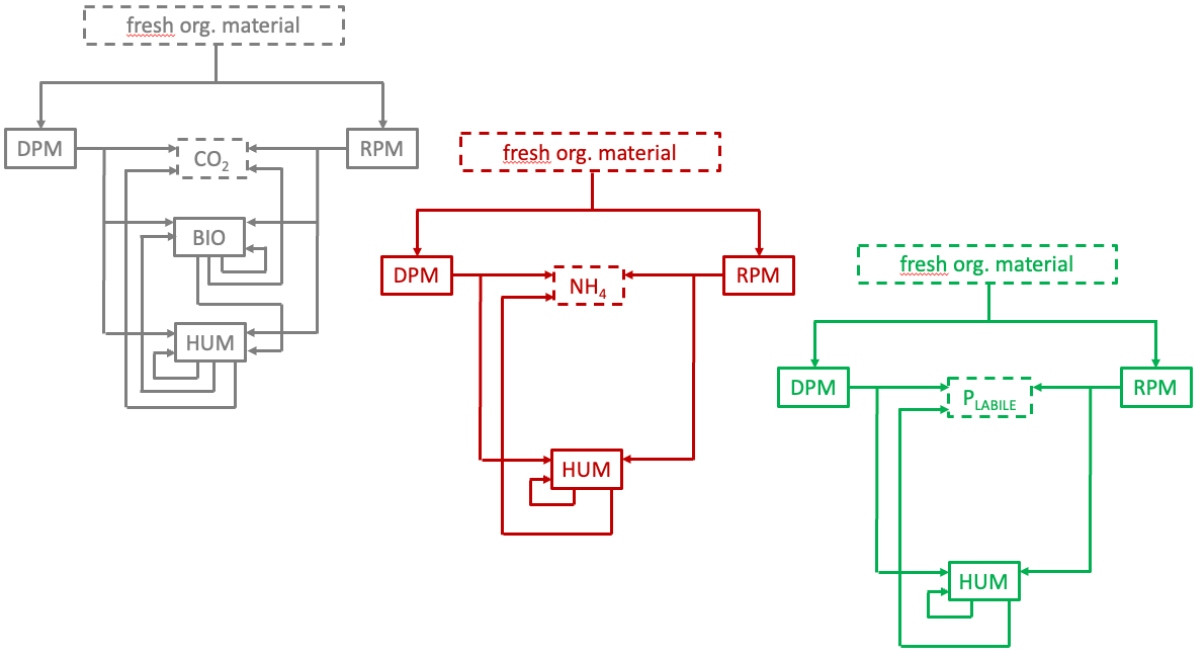

Fig. 4: Schematic turnover of organic carbon, nitrogen and phosphorus

The decomposition of organic P in the decomposable (DPM) and in the resistant plant material (RPM) as well as in the humus pool (HUM) is estimated as follows:

$$\frac{\partial P_{DPM}}{\partial t} = \left[(1 - f_h) f_e \frac{1}{r_o} - \frac{P_{DPM}}{C_{DPM}}\right] C_{DPM} \lambda_{DPM} \qquad (89)$$

where P_{DPM} [M P L^{-3} soil] is the phosphorus content in the decomposable plant material DPM pool, C_{DPM} [M C L^{-3} soil] is the carbon content of the DPM pool, λ_{DPM} [T^{-1}] is the DPM turnover rate and r_{oP} [-] represents the biomass C/P ratio, provided as model input. For consistency with the nitrogen turnover and with the RothC estimated carbon turnover, the dimensionless turnover efficiency f_e [-] is computed as 1-b/(b+1) (see Eq. 9, section 4.1), and the dimensionless humification facor f_h is equal to 0.54 (=RothC humification factor, please also see Eq. 15). A similar phosphorus turnover loop is assumed for the resistant plant material pool:

$$\frac{\partial P_{RPM}}{\partial t} = \left[(1 - f_h) f_e \frac{1}{r_o} - \frac{P_{RPM}}{C_{RPM}}\right] C_{RPM} \lambda_{RPM} \quad (90)$$

where P_{RPM} [M P L^{-3} soil] is the nitrogen content in the RPM pool, C_{RPM} [M C L^{-3} soil] is the carbon content of the RPM pool and λ_{RPM} [T^{-1}] is the RPM turnover rate. The net increase rate of phosphorus in the humus pool P_{HUM} [M P L^{-3} soil] is given by:

$$\frac{\partial P_{HUM}}{\partial t} = \frac{f_e f_h}{r_{oP}} (C_{DPM} \lambda_{DPM} + C_{RPM} \lambda_{RPM}) - C_{HUM} \lambda_{HUM} \quad (91)$$

Where C_{HUM} [M C L^{-3} soil] is the carbon content of the HUM pool and λ_{HUM} [T^{-1}] is the HUM turnover rate. The C and P turnover may result in net production or consumption of mineral P, which depends on the biomass C/P ratio and the C/P ratio of the three organic matter pools. The decrease of soil organic P in the three pools due to mineralization equals the increase of Phosphorus in the mineral form P_{min} [M P L^{-3} soil]:

$$\frac{\partial P_{min}}{\partial t} = \left[\frac{P_{DPM}}{C_{DPM}} - \frac{f_e}{r_o}\right] C_{DPM} \lambda_{DPM} + \left[\frac{P_{RPM}}{C_{RPM}} - \frac{f_e}{r_o}\right] C_{RPM} \lambda_{RPM} + C_{HUM} \lambda_{HUM} \quad (92)$$

The mineralized P is converted to a liquid phase concentration to be used as a source/sink term [M P L^{-3} water T^{-1}] for the labile mineral P pool P_{lab} [M P L^{-3} water]. The labile pool is assumed to be plant available and is represented as a liquid phase concentration in the solute transport equation. When the right side of the equation above is positive, P mineralization occurs. In case the right side is negative immobilization occurs and phosphorus mass is transferred from the liquid phase labile pool to the organic matter phosphorus pools. If immobilization occurs and the Phosphorus liquid phase concentration. In case the Phosphorus supply to the mineralization process is not sufficient, λ_{DPM} and λ_{RPM} are reduced by the

supply/demand ratio, which likewise affects organic C and N decomposition in the two plant material pools. For the supply from the liquid Phase phosphorus, the P_{DPM} pool is prioritized to the P_{RPM} pool, i.e. the remaining liquid phase Phosphorus may be consumed by the N_{DPM} decomposition first.

13.2 Mineral Phosphorus

The phosphorus available for plant uptake is also assumed to be mobile in the soil. The transport of the labile Phosphorus pool P_{lab} [M P L^{-3} water] is simulated with the Convection-Dispersion equation. Fertilizer application, plant uptake and leaching are computed with the solute transport module as available in the HYDRUS Version 4.17. One major process of P cycling in soils is sorption. Two options exist for AgroC to account for sorption of P. For the first option the HYDRUS physico-chemical routines for linear, Freundlich or Langmuir isotherms can be applied. The second option allows the sorption of labile P into mineral P pools active P_{ACT} [M P L^{-3} soil] and stable P_{STAB} [M P L^{-3} soil], as suggested in the classical mineral P cycling approach of Jones et al. (1984). This approach is based on instantaneous equilibrium and sorption/desorption rates between the labile P pool and the active P pool, and between the active P pool and the stable P pool.

The exchange rate R_{labact} [M P L^{-3} T^{-1}] between P_{lab} and P_{ACT} is computed from:

$$R_{labACT} = P_{lab} * \theta - P_{ACT} * \frac{PSP}{1-PSP} \quad (93)$$

Where θ is the soil water content, required to convert from the liquid-phase concentration to the soil volume related concentration of P_{ACT} and PSP [-] is the non-sorption coefficient, defined as the fraction of P that remains in the labile pool. The mass of P transferred via R_{labACT} is added to the P_{ACT} pool and substracted from P_{lab}, which is performed as a

source/sink term. The direction of exchange reverses, when P_{lab}*θ is smaller than P_{ACT}*PSP/(1-PSP) and R_{labACT} turns negative. In that case the reverse exchange is assumed to be much smaller and R_{labACT} is scaled down with the reverse rate modifier R_{rev} (default value=0.1).

At equilibrium, P_{STAB} is assumed to be larger than P_{ACT} and the corresponding exchange rate between the active and the stabe P pool $R_{ACTSTAB}$ [M P L^{-3} T^{-1}] is given as:

$$R_{ACTSTAB} = b_o * \left(Q_{STAB/ACT} * P_{ACT} - P_{STAB}\right) \quad (94)$$

Where b_o is an exchange coefficient and $Q_{STAB/ACT}$ is the stable to active pool ratio (default value=4.0). The mass of P transferred via $R_{ACTSTAB}$ is added to the P_{STAB} pool and substracted from P_{ACT}. Again, a reverse exchange, given when $P_{STAB} > Q_{STAB/ACT}$*P_{ACT}, is assumed to be slower and is scaled down with R_{rev}. Parameters PSP, $Q_{STAB/ACT}$, R_{rev}, and b_o are material-specific model input. PSP (between 0.05 and 0.75) can be calculated from the pedotransfer functions of Jones et al. (1984). Parameter b_o is 0.0076 for calcareous soils or =exp(-1.77*PSP-7.05) for all other soils.

13.3 Phosphorus uptake by roots

The uptake of Phosphorus closely follows the uptake scheme for Nitrogen with two exceptions: (i) the P content of the plant is not organ-specific but constant for the entire crop. (ii) the convective uptake can be limited to be a rather small proportion in relation to the diffusive uptake.

The potential uptake (=demand) P_p [M P L^{-2}] is computed from a dry matter nitrogen concentration for the crop, as provided in the plant parameter input file against development stage DVS. The potential P uptake rate [M P L^{-2} T^{-1}] is computed as:

$$\frac{\partial P_p}{\partial t} = W_{tot} * XPC_{tot} - P_{act} \quad (95)$$

Where W_{tot} [M DM L^{-2}] is the accumulated dry matter of the total crop, XPC_{tot} [M N M^{-1} DM] is the potential dry matter nitrogen P concentration of the crop and P_{act} [M P L^{-2}] is the Phosphorus accumulated in the plant over the growing season. Uptake is supposed to occur convective, with the root water uptake, and diffusive.

The diffusive uptake rate [M P L^{-2} T^{-1}] is calculated as:

$$\frac{\partial P_{dif}}{\partial t} = \int_0^{R_d} \frac{2*\pi*R_{dens}*RORAD*\tau*P_{lab}*\theta}{D_0} dx \quad (96)$$

Where P_{dif} [M P L^{-2}] is the diffusive uptake, R_{dens} [L L^{-3}] is root density at a specific depth, RORAD [L] is the mean root radius, τ [L^2 T^{-1}] is the Phosphorus diffusion coefficient in water for a given water content, D_0 [L^{-1}] is the travel distance resistance between bulk soil solution and root and dx is the depth increment [L]. Please note that uptake P_{dif} and $P_{conv,act}$ are related to soil volume, and not to water volume. As for the nitrogen uptake, Root density over depth is calculated by scaling the root density at the surface W_{0dens} [L L^{-3}] with the relative root density RRD [-]. Convective P uptake only occurs when diffusive uptake does not supply the entire crop P demand. The potential convective uptake rate [M P L^{-2}] is given by:

$$\frac{\partial P_{conv,pot}}{\partial t} = \int_0^{R_d} S_w * P_{lab} * dx \quad (97)$$

Where R_d is actual root depth [L], *dx* is the element thickness [L] and S_w [L^3 L^{-3} T^{-1}] is the root water uptake sink term. The actual convective P uptake $P_{conv,act}$ [M P L^{-2}] is given by:

$$P_{conv,act} = min\left(P_{conv,pot}, L_{CD} * \left(P_{conv,pot} + P_{diff}\right)\right) \quad (98)$$

Where the input parameter L_{CD} [-] is the limit of the fraction of $P_{conv,act}$ in relation total P uptake. The sum of P_{diff} and $P_{conv,act}$ equals the total uptake P_{act} [M P L^{-2}] and is simulated as a sink term in the solute transport routine, where uptake can never exceed the available liquid phase Phosphorus mass.

The reduction factor P_{RED} [-] for crop growth according to limited P uptake varies between 0 and 1 and is computed according to the APEX approach suggested by Williams and Izaurralde (2008):

$$s_{ns} = 200 * \left(\frac{APC_{tot}}{XPC_{tot}}\right) \quad (99)$$

$$P_{RED} = \frac{s_{ns}}{s_{ns} + e^{(4.056 - 0.0535 * s_{ns})}} \quad (100)$$

Where APC_{tot} [M N M^{-1} DM] is the current P content of the crop, given as P_{act}/W_{tot}.

14. Harvest residues

Aboveground harvest residues are assumed to be incorporated directly after the given harvest date up to the plowing depth P_{dep} [L]. The amount of aboveground residues in terms of carbon $R_{C,a}$ [M C L^{-2}], nitrogen $R_{N,a}$ [M N L^{-2}] and phosphorus $R_{P,a}$ [M P L^{-2}] is estimated in dependence of the crop type. For Winter wheat, spring wheat and maize $R_{C,a}$ is calculated as:

$$R_{C,a} = F_{st} * W_{st} * 0.493 \quad (101)$$

Where F_{st} [-] is the fraction of the stem that is incorporated into the soil (=0.25 for winter wheat and spring wheat and =0.1 for maize), W_{st} [M DM L^{-2}] is the dry weight of the stem and 0.493 kg C kg^{-1} DM is the stem-specific dry matter carbon content (Goudriaan et al., 1997). The amount of aboveground N residues for cereals and maize is calculated as:

$$R_{N,a} = F_{st} * AN_{st} \quad (102)$$

Where AN_{st} is the the amount of N stored in the stem [M N L^{-2}]. Correspondingly, the amount of aboveground P residues for cereals and maize is calculated as:

$$R_{P,a} = F_{st} * AP_{st} \quad (103)$$

Where AP_{st} is the amount of P stored in the stem [M P L^{-2}]. For potato and sugar beet all of the leaf and stem biomass is assumed to be incorporated into the soil. In terms of C this is calculated as:

$$R_{C,a} = W_{st} * 0.493 + \left(W_{lvg} + W_{lvd}\right) * 0.459 \quad (104)$$

Where W_{lvg} [M DM L^{-2}] and W_{lvd} [M DM L^{-2}] are the dry weight of the green and dead leaves, respectively, and 0.459 kg C kg^{-1} DM is the leaf-specific dry matter carbon content (Goudriaan et al., 1997). In terms of nitrogen the harvest residues input for potato and sugar beet is calculated as:

$$R_{N,a} = AN_{st} + AN_{lv} \quad (105)$$

Where AN_{lv} is the amount of N stored in the leaves [M N L^{-2}]. In terms of phosphorus the harvest residues input for potato and sugar beet is calculated as:

$$R_{P,a} = AP_{st} + AP_{lv} \quad (106)$$

Where AP_{lv} is the amount of P stored in the leaves [M N L^{-2}]. The depth-specific input by aboveground harvest residues [M L^{-3}] is assumed to be equally distributed over depth (down to the plowing depth) and is estimated by dividing the total amount of aboveground harvest residues [M L^{-2}] by plowing depth [L].

Belowground residues area also assumed to occur directly after the harvest date. The amount of depth-specific belowground residues in terms of carbon $R_{C,b}$ [M C L^{-3}] is calculated in dependence of the final root profile as:

$$R_{C,b} = RRD * W_{rt} * \frac{0.467}{dz} \quad (107)$$

Where RRD [-] is the node-specific relative root length density, W_{rt} [M DM L^{-2}] is the dry matter weight of the roots, 0.467 kg C kg^{-1} DM is the root-specific dry matter carbon content

(Goudriaan et al., 1997) and dz [L] is the thickness of the layer associated to the spatial discretization node at that specific soil depth.

Node-specific belowground harvest residues in terms of nitrogen $R_{N,b}$ [M N L^{-3}] are estimated as:

$$R_{N,b} = RRD * \frac{AN_{rt}}{dz} \quad (108)$$

Where AN_{rt} [M N L^{-2}] is the amount of N stored in the roots. Analogous, node-specific belowground harvest residues in terms of phosphorus $R_{P,b}$ [M N L^{-3}] are estimated as:

$$R_{P,b} = RRD * \frac{AP_{rt}}{dz} \quad (109)$$

Where AP_{rt} [M P L^{-2}] is the mass of P stored in the roots. Total node-specific harvest residues input is given as the sum of the aboveground and belowground inputs at a certain depth and it is split into 59% for the DPM type C, N and P pool and 41% goes into the RPM-type C, N and P pools, as suggested by Coleman and Jenkinson, 2008.

References

Allen, R.G., Pereira, L.S., Raes, D., Smith, M., 1998. Crop Evapotranspiration. Guidelines for computing crop water requirements. FAO Irrigation and Drainage Paper No. 56. Food and Agriculture Organization of the United Nations (FAO), Rome. 300 pp.

Aulakh, M.S, Doran, J.W., Mosier, A.R., 1992. Soil denitrification significance, measurements and effects of management. Advances in Soil Science 18, 2-42.

Anslow, R.C., Green, J.O., 1967. The seasonal growth of pasture grasses. J Agr Sci 68, 109-122.

Barrett, P.D., Laidlaw, A.S., Mayne, C.S., 2004. An evaluation of selected perennial ryegrass growth models for development and integration into a pasture management decision support system. J Agr Sci 142, 327-334. DOI 10.1017/s0021859604004289.

Bauer, J., Herbst, M., Huisman, J.A., Weihermüller, L., Vereecken, H., 2008. Sensitivity of simulated soil heterotrophic respiration to temperature and moisture reduction functions. Geoderma 145 (1-2), 17-27. DOI 0.1016/j.geoderma.2008.01.026.

Bauer, J., Weihermüller, L., Huisman, J.A., Herbst, M., Graf, A., Séquaris, J.-M., Vereecken, H., 2012. Inverse determination of heterotrophic soil respiration response to temperature and water content under field conditions. Biogeochemistry 108 (1-3), 119-134. DOI 10.1007/s10533-011-9583-1.

Björkman, O., Demmig, B., 1987. Photon yield of O_2 evolution and chlorophyll fluorescence characteristics at 77 K among vascular plants of diverse origins. Planta 170, 489-504.

Coleman, K., Jenkinson, D.S., 2008. RothC-26.3. A model for the turnover of carbon in soil. Model description and windows users guide. IACR-Rothamsted, Harpenden. 47 pp.

Collatz, G.J., Ball, T., Grivet, C., Berry, J.A., 1991. Physiological and environmental regulation of stomatal conductance, photosysnthesis and transpiration: a model that includes a laminar boundary layer. Agricultural and Forest Meteorology 54, 107-136.

Couvreur, V., Vanderborght, J., Javaux, M., 2012. A simple three-dimensional macroscopic root water uptake model based on the hydraulic architecture approach. Hydrol. Earth Syst. Sci. 16, 2957-2971.

Del Grosso, S.J., et al. 2000. General model for N_2O and N_2 gas emissions from soils due to dentrification. Global Biogeochem. Cycles 14, 1045-1060.

Farquhar, G.D., von Caemmerer, S., Berry, J.A., 1980. A biochemical model of photosynthetic CO_2 assimilation in leaves of C_3 species. Planta 149, 78-90.

Feddes, R.A., Kowalik, P.J., Zaradny, H., 1978. Simulation of field water use and crop yield. Simulation Monographs, Wageningen, 188 pp.

Firestone, M.K., Davidson, E.A. 1989. Exchange of Trace Gases between Terrestrial Ecosystems and the Atmosphere. In: M.O. Andreae and D.S. Schimel (Editors). John Wiley and Sons, pp. 7-21.

Gonzales, B., Boucaud, J., Salette, J., Langlois, J., Duyme, M., 1989. Changes in stubble carbohydrate content during regrowth of defoliated perennial ryegrass (*Lolium perenne* L.) on two nitrogen levels. Grass Forage Sci 44 (4), 411-415. DOI 10.1111/j.1365-2494.1989.tb01940.x.

Goudriaan, J., van Keulen, H., van Laar, H.H., 1997. Crop growth model for potential production (SUCROS1), in: van Laar, H.H., Goudriaan, J., van Keulen, H. (Eds.), SUCROS97: Simulation of crop growth for potential and water-limited production situations. As applied to spring wheat. Quantitative Approaches in Systems Analysis, AB-DLO, Wageningen, pp. 1-20.

Herbst, M., Hellebrand, H.J., Bauer, J., Huisman, J.A., Šimůnek, J., Weihermüller, L., Graf, A., Vanderborght, J., Vereecken, H., 2008. Multiyear heterotrophic soil respiration: Evaluation of a coupled CO_2 transport and carbon turnover model. Ecol Model 214 (2-4), 271-283. DOI 10.1016/j.ecolmodel.2008.02.007.

Hopkins, F., Gonzalez-Meler, M.A., Flower, C.E., Lynch, D.J., Czimczik, C., Tang, J., Subke, J.-A., 2013. Ecosystem-level controls on root rhizosphere respiration. New Phytol 199 (2), 339-351. DOI 10.1111/nph.12271.

Huwe, B., Van der Ploeg, R., 1988. Modelle zur Simulation des Stickstoffhaushaltes von Standorten mit Unterschiedlicher landwirtschaftlicher Nutzung. Eigenverlag des Instituts für Wasserbau der Universität Stuttgart, Heft 69. 213 pp.

Kristensen, A.H., Thorbjørn, A., Jensen, M.P., Pedersen, M., Moldrup, P., 2010. Gas-phase diffusivity and tortuosity of structured soils. J Contam Hydrol 115 (1-4), 26-33. DOI 10.1016/j.jconhyd.2010.03.003.

Kuzyakov, Y., 2006. Sources of CO_2 efflux from soil and review of partitioning methods. Soil Biol Biochem 38 (3), 425-448. DOI 10.1016/j.soilbio.2005.08.020.

Leafe, E.L., Stiles, W., Dickinson, S.E., 1974. Physiological processes influencing the pattern of productivity of the intensively managed grass sward. Sectional Papers, 12th International Grassland Congress (congress proceedings - June 11-20, 1974), Vol. 1, Part I, 442-457.

Lee, J.-E., Berry, J.A., Van der Tol, C., Yang, X, Guanter, L.,Damm, A., Baker, J., Frankenberg, C., 2015. Simulations of chlorophyll fluorescence incorporated into the Community Land Model version 4. Global Change Biology 21, 3469-3477.

Li, C., Aber, J., Stange, F., Butterbach-Bahl, K., Papen, H. 2000. A process-oriented model of N_2O and NO emissions from forest soils: 1. Model development. J. Geophys. Res. 105(D4), 4369-4384.

McIsaac, D.M., Watts, D., 1985. Users guide to NITWAT – a nitrogen and water management model. Agr. Eng. Dept. University of Nebraska, Lincoln, Nebraska, United States of America

Moldrup, P., Olesen, T., Gamst, J., Schjonning, P., Yamaguchi, T., Rolston, D.E., 2000a. Predicting the Gas Diffusion Coefficient in Repacked Soil Water-Induced Linear reduction Model. Soil Sci. Soc. Am. J. 64, 1588-1594.

Moldrup, P., Olesen, T., Schjonning, P., Yamaguchi, T., Rolston, D.E., 2000b. Predicting the gas diffusion coefficients in undisturbed soil from soil water characteristics. Soil Sci. Soc. Am. J. 64, 94-100.

Palosuo, T., Foereid, B., Svensson, M., Shurpali, N., Lehtonen, A., Herbst, M., Linkosalo, T., Ortiz, C., Todorovic, G.R., Marcinkonis, S., Li, C., Jandl, R., 2012. A multi-model comparison of soil carbon assessment of a coniferous forest stand. Environ Modell Softw 35, 38-49. DOI 10.1016/j.envsoft.2012.02.004.

Parsons, A.J., 1988. The effects of season and management on the growth of grass swards, in: Jones, M.B., Lazenby, A. (Eds.), The grass crop. The physiological basis of production. Chapman and Hall, London, New York, pp. 129-177.

Prud'homme, M.-P., Gonzalez, B., Billard, J.-P., Boucaud, J., 1992. Carbohydrate content, fructan and sucrose enzyme activities in roots, stubble and leaves of ryegrass (*Lolium perenne* L.) as affected by source/sink modification after cutting. J Plant Physiol 140, 282-291.

Robson, M.J., Ryle, G.J.A., Woledge, J., 1988. The grass plant - its form and function, in: Jones, M.B., Lazenby, A. (Eds.), The grass crop. The physiological basis of production. Chapman and Hall, London, New York, pp. 25-83.

Rutter, A.J., Kershaw, K.A., Robins, P.C., Morton, A.J., 1971. A predictive model of rainfall interception in forests, 1. Derivation of the model from observations in a plantation of Corsican pine. Agr Meteorol 9, 367-384. DOI 10.1016/0002-1571(71)90034-3.

Schapendonk, A.H.C.M., Stol, W., van Kraalingen, D.W.G., Bouman, B.A.M., 1998. LINGRA, a sink/source model to simulate grassland productivity in Europe. Eur J Agron 9, 87-100. DOI 10.1016/S1161-0301(98)00027-6.

Šimůnek, J., Suarez, D.L., 1993. Modeling of carbon dioxide transport and production in soil 1. Model development. Water Resour Res 29 (2), 487-497. DOI 10.1029/92WR02225.

Šimůnek, J., Suarez, D.L., Šejna, M., 1996. The UNSATCHEM Software Package for simulating the one-dimensional variably saturated water flow, heat transport, carbon dioxide production and transport, and multicomponent solute transport with major ion equilibrium and kinetic chemistry, Version 2.0. Research Report No. 141. U.S. Salinity Laboratory, Agricultural Research Service, U.S. Department of Agriculture, Riverside, California, 186 pp.

Spitters, C.J.T., van Keulen, H., van Kraalingen., D.W.G., 1989. A simple and universal crop growth simulator, SUCROS87, in: Rabbinge, R., Ward, S.A., van Laar, H.H., (Eds.), Simulation and systems management in crop protection. Simulation Monographs 32, PUDOC, Wageningen, pp. 147-181.

Supit, I., Hooijer, A.A., van Diepen, C.A., 1994. System description of the WOFOST 6.0 Crop Simulation Model implemented in CGMS. Volume 1: theory and algorithms. EUR 15956 EN, Joint Research Centre, European Commission, Luxembourg. 146 pp.

Swinnen, J., van Veen, J.A., Merckx, R., 1995. Carbon fluxes in the rhizosphere of winter wheat and spring barley with conventional vs integrated farming. Soil Biol Biochem 27 (6), 811-820. DOI 10.1016/0038-0717(94)00230-X.

Vanclooster, M., Viaene, P., Diels, J., Christiaens, K., 1995. WAVE: A mathematical model for simulating water and agrochemicals in the soil and vadose environment: Reference and user's manual (release 2.0). Institute for Land and Water Management, Katholieke Universiteit, Leuven, Belgium. 154 pp.

Vereecken, H., Vanclooster, M., Swerts, M., Diels, J., 1991. Simulating water and nitrogen behaviour in soil cropped with winter wheat. Fert. Res. 27: 233-243.

Weihermüller, L., Huisman, J.A., Graf, A., Herbst, M., Séquaris, J.-M., 2009. Multistep outflow experiments to determine soil physical and carbon dioxide production parameters. Vadose Zone J 8 (3), 772-782. DOI 10.2136/vzj2008.0041.

Williams, J.R., Izaurralde, R.C., 2008. The APEX model. APEX_EPIC_BRCREPORT2008-02_2.pdf